Experimental Mechanics (2016) 56:1411–1426
DOI 10.1007/s11340-016-0181-y

A Hybrid Wavelet Based–Approach and Genetic Algorithm to Detect Damage in Beam-Like Structures without Baseline Data

S.A. Ravanfar[1] · **H. Abdul Razak**[1] · **Z. Ismail**[2] · **S.J.S. Hakim**[1]

Received: 12 January 2015 / Accepted: 25 May 2016 / Published online: 6 June 2016

Abstract This paper proposes an optimized damage identification method in beam-like structures using genetic algorithm (GA) without baseline data. For this purpose, a vibration-based damage identification algorithm using a damage indicator called 'Relative Wavelet Packet Entropy' (RWPE) was implemented to determine the location and extent of damage. The procedure does not require vibration signals from an undamaged structure because the method of comparing signals from different locations in the existing state was found to be effective. To ameliorate the algorithm, GA was utilized to identify the best choice for "mother wavelet function" and "decomposition level" of the signals by means of the fundamental fitness function to optimize the algorithm. This resulted in the high accuracy of the damage identification algorithm. In addition, this method has eliminated the difficulties in selecting the type of mother wavelet function for damage identification purposes. To investigate the robustness and accuracy of the proposed method, numerical examples and experimental cases with different damage depths were considered and conducted. The results demonstrated that the proposed method has great potential in the identification of damage location and depth of cut in beam-like structures since it does not require the recorded data from an undamaged beam as a baseline for damage detection. Moreover, the relationship between damage location and depth of damage has been evaluated and results showed that the algorithm can be applied to actual structures.

Keywords Relative wavelet packet entropy · Genetic algorithm · Damage detection · Vibration signal

✉ H. Abdul Razak
hashim@um.edu.my

[1] StrucHMRS Group, Department of Civil Engineering, Faculty of Engineering, University of Malaya, 50603 Kuala Lumpur, Malaysia

[2] Department of Civil Engineering, Faculty of Engineering, University of Malaya, 50603 Kuala Lumpur, Malaysia

Introduction

Damages such as notches, cracks and delaminations, are inevitable in aerospace, mechanical and civil engineering structures and may occur during their service life. To ensure structural integrity and prevent structural damages from deteriorating at an alarming rate, advanced structural health monitoring (SHM) techniques are required and have been widely studied during the last few decades [1]. Vibration-based analysis has been reported as a promising method for SHM [2, 3]. The premise of vibration-based SHM is that the dynamic characteristics of a structure are a function of its physical properties. Therefore, changes in these physical properties, such as reduction in stiffness resulting from localized structural damage will cause observable changes in the dynamic characteristics of the structure.

In recent years, the wavelet transform has emerged as a promising tool for structural health monitoring and damage detection due to its potential characteristics such as singularity detection, good handling of noisy data and being very informative about damage location/time. Consequently, many studies on damage detection have focused on the wavelet transform scheme. Kim and Melhem [4] have presented a considerable amount of literature on the subject, with particular application to crack detection of beam-like structures.

Recent studies in this context can be categorized into two groups based on the dependence on healthy data; in the first group, researchers only employed the spatial data of the

defective structure while in the second group, data of both undamaged and damaged structures were required.

In the first group of references [5–10], although the frequently considered damaged structure was a beam, other elements such as plane frames [11] and plates as a bi-dimensional structure [12–14] were also considered. Even though the signal to be processed by the wavelet transform is frequently the mode shape of the damaged structure, Wang and Deng [15] employed other spatial data like displacement and strain measurements of a cracked beam subjected to impact loading to locate damage by sensing local perturbations at sites of damage, and then considering the displacement response of a plate under in-plane stress. Zhong and Oyadiji [16] developed an approach based on the difference between two sets of detailed coefficients by using stationary wavelet transform (SWT) for crack detection in beam-like structures. The main limitation of the method is its applicability in symmetric beams. Subsequently, Zhong and Oyadiji [17] proposed a technique based on the difference of the continuous wavelet transforms (CWTs) of two sets of mode shape data which correspond to the left half and the right half of the modal data of a cracked simply-supported beam. A continuous relative wavelet entropy (CRWE)–based baseline-free damage algorithm was proposed by Lee et al. [18] for truss bridge structures. The damage-sensitive index (DSI) of each sensor's location was defined by CRWE measurements of different sensor-to-sensor pairs. The CRWE was reported to be able to detect damage but with considerably large computation cost for the real time monitoring algorithm. Among the baseline-free methods, Mikami et al. [19] employed variation between two sets of power spectrum density magnitudes calculated by means of wavelet packet decomposition components of two sets of acceleration response of the damaged beam. The method was able to examine the effect of damage location, wavelet type and decomposition level in the steel beam.

With regard to the second group, the procedures in these articles were similar to those of the first group except that healthy data was employed in the baseline. Wavelet coefficients of the original signal were generally subtracted from the damaged coefficients [20–24]. In a different study, Han et al. [25] proposed a damage detection index called the wavelet packet energy rate index for the damage detection of beam structures. The simulated and experimental studies demonstrated that the wavelet packet transform-based energy rate index was a good index candidate that was sensitive to local structural damage. However, a significant limitation of this method is that a reliable reference structural model for the healthy condition was required. Ren and Sun [26] proposed damage identification features such as wavelet entropy, relative wavelet entropy and wavelet-time entropy, which were defined and investigated to detect and locate damage through the vibration signals measured from the undamaged (reference) and damaged structures. Neural networks have been established as a powerful tool for pattern recognition and damage identification, especially when combined with wavelet transform. Yam et al. [27] proposed a method based on the energy variation of the wavelet packet components of the structural vibration response and identification of structural damage status using artificial neural networks (ANNs) before and after the occurrence of structural damage. Diao et al. [28] proposed a two-step structural damage detection approach based on wavelet packet analysis and neural networks. The significant disadvantage of the methods included in the second group is the absence of healthy data for many structures, especially the older ones. Hence, many research works have been carried out to develop methods requiring only damaged data.

Experimental noise is inevitable for real data, thus its influence on wavelet coefficients have been widely reported. Law et al. [29] developed the sensitivity-based damage detection method based on the wavelet packet energy of the measured accelerations. The method identified damage of a structure from a few measurement locations with no sensitivity to noise. Cruz and Salgado [30] evaluated six vibration-based damage detection methods including curvature, COMAC, damage index, continuous wavelet transform, discrete wavelet analysis and wavelet packet signature for various crack depth, damage extension and noise level in a bridge. Levels of noise sensitivity of the evaluated methods were found different while wavelet packet signature was more tolerant of the noise. Vafaei et al. [31] proposed a method based on artificial neural networks and wavelet transform for identifying seismic-induced damage of cantilever structures. Results showed that the noise intensity had negligible effect on damage identification.

In the last two decades, genetic algorithms (GAs) [32] have been recognized as promising intelligent search techniques for difficult optimization problems. GAs are stochastic search techniques based on the mechanism of natural selection and natural evolution. Hao and Xia [33] applied a genetic algorithm with real number encoding to identify the structural damage by minimizing the objective function, which directly compares the changes in the measurements before and after damage. Three different criteria were considered, namely, the frequency changes, the mode shape changes, and a combination of the two. The algorithm did not require an accurate analytical model and gave better damage detection results for the beam than the conventional optimization method. Vakil-Baghmisheh et al. [34] successfully applied the genetic algorithm to predict the size and location of a crack in a cantilever beam by minimizing the cost function, which was based on the difference of measured and calculated natural frequencies. Rafiee et al. [35] has suggested a technique for choosing the number of neurons in the hidden layer and wavelet functions using an intelligent fault identification system.

GA and ANNs were employed to identify the failure type of a complex gear box system.

In this study, a new approach for optimized damage identification in beam-like structures is presented and applied to a damaged steel beam. This new approach is based on wavelet packet transform (WPT) which reduces the redundant information of data and enables faster computation. The WPT was combined with entropy analysis to determine an effective damage indicator, RWPE, to obtain information about the relative energy correlated with various frequency bands presented in structural response segments for investigating the location and severity of damage. The method does not require the baseline data from an undamaged beam because of its effective comparative approach of response signals of different locations.

The choice of the mother wavelet function and decomposition level of signal is the most crucial challenge in wavelet analysis. In order to employ the dyadic discrete wavelet transform, Daubechies (DB) wavelets which have been chosen from the orthogonal wavelets family was employed in this research. DB wavelets have the significant advantage of matching the transient components in vibration signals.

The order of the mother wavelet function is another subject matter in wavelet analysis. This drawback has been previously specified by trial-and-error procedure based on inherent characteristics of the data. Therefore, GA was employed to ameliorate this problem and to search for the optimal Daubechies order and decomposition level of the signal. Both numerical simulation and experimental data with different damage scenarios revealed that the proposed algorithm has a great potential in damage identification of beam-like structures.

Wavelet Packet

Wavelet Packet Decomposition (WPD)

Wavelet transform (WT) is a relatively new signal processing method efficient for multi-resolution analysis and local features of non-stationary signals. It can be considered as an extension of the traditional Fourier transform with modifiable window size and location [36]. Wavelet packet transform (WPT) could be considered as an extension of the WT which provides a complete level-by-level time-frequency decomposition. In addition, it can give a rich structure that permits adaptation to a particular signal. WPT also enables multi resolution damage detection since it can localize multi-frequency bands in the time domain. More details can be found in the textbook by Mallat [37]. The wavelet packet function is defined as

$$\psi^{\mathrm{i}}_{\mathrm{j,k}}(\mathrm{t}) = 2^{j/2}\psi^{i}\left(2^{j}t-k\right) \quad i = 0,1,2,\ldots,2^{j}-1 \tag{1}$$

where a wavelet packet $\psi^{\mathrm{i}}_{\mathrm{j,k}}(\mathrm{t})$ is a function of three indices with integers i, j and k, denoting the modulation, the scale and the translation parameter, respectively. Moreover, $\psi^{0}(t)=\varphi(t)$ for $i=0$ and $\psi^{1}(t)=\psi(t)$ for $i=1$. The wavelet $\varphi(t)$ is called the scaling function and $\psi(t)$ is called the mother wavelet function. The wavelets ψ^{i} for $i>1$ are obtained from the scaling function and the mother wavelet function as:

$$\psi^{2i} = \sqrt{2}\sum\nolimits_{k} h(k)\psi^{i}(2t-k) \tag{2}$$

$$\psi^{2i+1} = \sqrt{2}\sum\nolimits_{k} g(k)\psi^{i}(2t-k) \tag{3}$$

where g(k) and h(k) are quadrature mirror filters associated with the mother wavelet function and the scaling function. In this work, the measured dynamic structural response is decomposed into wavelet component functions. While the level of decomposition is j, 2^{j} WPD components can be obtained. The original signal can be expressed as a summation of WPD components as,

$$f(t) = \sum\nolimits_{i=1}^{2^{j}} f^{i}_{j}(t) \tag{4}$$

where t is time lag; $f^{i}_{j}(t)$ is the WPD component signal that can be represented by a linear combination of wavelet packet functions as follows:

$$f^{i}_{j}(t) = \sum\nolimits_{k=-\infty}^{\infty} C^{i}_{j,k}\psi^{i}_{j,k}(t) \tag{5}$$

where $C^{i}_{j,k}$ is the wavelet packet coefficient and can be calculated from

$$C^{i}_{j,k} = \int_{-\infty}^{\infty} f(t)\psi^{i}_{j,k}(t)dt \tag{6}$$

WPT offers good time resolution in the high-frequency range of a signal and good frequency resolution in the low-frequency range of the signal. In general, the wavelet-based methods are completely reliant on the mother wavelet function. Ingrid Daubechies invented what is called ‘compactly supported orthonormal wavelets’– thus making discrete wavelet analysis practical [38]. In structural health monitoring, wavelet functions in the Daubechies family are often chosen for signal analysis and synthesis because it satisfies the two crucial requirements, i.e., the orthogonality of local basis functions and second or higher-order accuracy is generally determined by trial and error. Apart from the reliance on the mother wavelet function, the wavelet-based methods link up with the decomposition level at which the wavelet analysis must be carried out. The specification of an appropriate level is not possible in advance and depends on a wide range of parameters which include the characteristics of the structure, the nature of the signal and the type, location and severity of the damage, etc. Several researchers have suggested to try different decomposition levels [11, 19, 39–42]. In other words,

there is no computational logic behind the selection of Daubechies order which is therefore considered to be optimized for damage identification in this study. It is of paramount significance to note that calculation of the wavelet coefficients is directly dependent on the shape of the mother wavelet such that the correlation between mother wavelet and signal is calculated as wavelet coefficients. This study aims to propose an effectual method to eliminate the shortcoming arising from the similarity of Daubechies family functions with adjacent order (e.g., DB4 and DB5), as depicted in Fig. 1, as well as acquiring higher precision and efficiency by introducing a damage indicator.

Damage Indicator and Identification Procedure

The wavelet packet component energy is a suitable tool to identify and characterize a specific phenomenon of signal in the time-frequency domain. It has been shown by Yen and Lin [43] that the energy stored in a specific frequency band at a certain level of WPD provides a greater potential for signal feature than the coefficients alone. Sun and Chang [41] conducted a comparative study on the sensitivity of four damage indices based on variations of frequency, mode shape, flexibility and wavelet packet energy and deduced that wavelet packet energy based index has a high potential to capture the reduction in structural stiffness. The sensitivity of the wavelet packet transform component energy with regard to local change in the system parameters was derived by Law et al. [29]. Ren et al. [39] has studied the application of wavelet packet energy variation based damage detection method in bridge shear connector monitoring.

The wavelet packet energy E_f of a signal is defined as

$$E_f = \int_{-\infty}^{\infty} f^2(t)dt = \sum_{m_1=1}^{2^j}\sum_{m_2=1}^{2^j}\int_{-\infty}^{\infty} f_j^{m_1}(t)f_j^{m_2}(t)dt \tag{7}$$

where $f_j^{m_1}$ and $f_j^{m_2}$ stand for decomposed wavelet components. The total signal energy can be expressed as the summation of wavelet packet component energies when the mother wavelet is orthogonal:

$$E_f = \times\sum_i^{2^j} E_{f_j^i} = \sum_{i=1}^{2^j}\int_{-\infty}^{\infty} f_j^i(t)^2 dt \tag{8}$$

Then, the energy ratio of each wavelet coefficient can be written as

$$p_{ij} = \frac{E_{f_j^i}}{E_f} \tag{9}$$

The p_{ij} values correspond to a ratio of the energy of a particular coefficient $E_{f_j^i}$ to the total energy. The p_{ij} value acts like a probability distribution of the energy. Therefore, the p_{ij} values sum to one.

The Shannon entropy represents the amount of information which is also often used as a measure of the extent of signal energy concentration in the time-frequency domain. Ren and Sun [26] applied the concept of the wavelet entropy to structural damage detection problems. The wavelet entropy spectra represent the level of order/disorder of vibration signals [44]. According to the Shannon entropy theory and wavelet energy ratio defined above, wavelet packet entropy is given as

$$S_{WPE} = S_{WPE}(p) = -\sum_j\sum_i p_{ij}.lnp_{ij} \tag{10}$$

in which the range of j depends on the selection of decomposition level of a signal and it is a constant value in the case of the WPT. The damage detection problem can be formulated through the changes in the wavelet packet entropy of damaged structures to detect the location and severity of damage. To identify the change of vibration signals of a structure, the relative wavelet packet entropy (RWPE) is defined as:

$$S_{RWPE}^k\left(p^{\alpha k}\middle|p^{\beta k}\right) = \sum_j\sum_i\left|p_{ij}^{\alpha k}\ln\left(\frac{p_{ij}^{\alpha k}}{p_{ij}^{\beta k}}\right)\right| \quad k = x,\ y, z \tag{11}$$

where α and β denote locations where the data is measured. It is notable that accelerations measured in the same direction should be used in computations of RWPE. Since damage at a location affects vibration signals in every direction, the baseline-free damage indicator, F_{RWPE}, at a location "α" has been defined as:

$$F_{RWPE} = \sum_{k=1}^{x,y,z}\sum_{\beta=1}^{N} S_{RWPE}^k\left(p^{\alpha k}\middle|p^{\beta k}\right) \tag{12}$$

In equation (12), N indicates the whole number of locations corresponding to the number of sensors. Based on this equation, the vibration signal at a reference point is compared with signals from other measured points, and thus allows the possibility of damage detection without using data from the undamaged state.

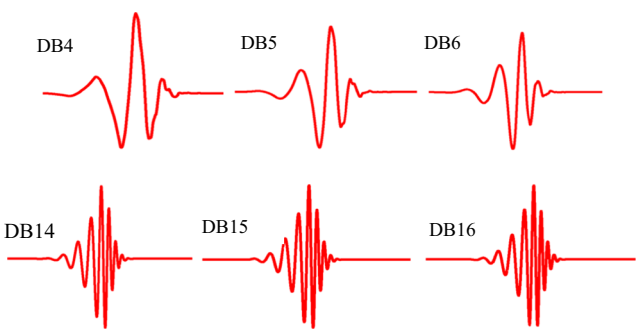

Fig. 1 Order of Daubechies wavelet function

In order to determine the location of damage clearly, it is proposed to establish a threshold value for damage indicators through applying statistical properties and the one-side confidence limit of the damage indicators from successive measurements [25, 45]:

$$UL = \mu + Z_{\overline{\alpha}}\left(\frac{\sigma}{\sqrt{N}}\right) \tag{13}$$

in which N stands for the whole number of sensors distributed in a structure where a total of N F_{RWPE} values can be achieved. When the mean value and the standard deviation of these F_{RWPE} values are represented as μ and σ, UL expresses the one-side $(1-\overline{\alpha})$ upper confidence limit for these F_{RWPE} values, while $Z_{\overline{\alpha}}$ is the value of a standard normal distribution with zero mean and unit variance such that the cumulative probability is 100 $(1-\overline{\alpha})$ %. This limit can be considered as a threshold value which is an entrance point of possible abnormality in the damage indicator indicated by the F_{RWPE}. The advantage of this damage identification is that setting of the threshold value is according to statistical properties of the damage indicator measured with sensors. The location of sensors whose the F_{RWPE} values exceed the threshold will represent where possible damage takes place.

Numerical Investigation

Finite Element Method Analysis

To verify the suitability of the proposed damage identification method, numerical simulations were conducted on three I-section steel beams with a span length of 3 m and simulated damage elements, as shown in Fig. 2. Beam 1 was the single damage scenario with damage located at point 5 while Beam 2 had two damage points at locations 11 and 13. Beam 3 had three damage points induced at the middle of the beam and at locations 10 and 12. Damage was simulated in the form of a notch with a 3 mm width. Damage depth for all beams was increased gradually from 3 mm up to 75 mm as depicted in Fig. 2(a). The mass density and modulus of elasticity of the beam material were 7850 kg/m^3 and 2.1 GPa, respectively, and the Poisson's ratio was 0.33.

The time history acceleration responses of beams were computed by the finite element analysis package (ABAQUS) using transient dynamic analysis. To simulate an impulse load, the force-time history was applied at location 14 on the beam. The node acceleration responses of the beam under the impulse load were obtained from sixteen locations on the top flange as shown in Fig. 2(b) at a sampling frequency of 2000 Hz to identify the characteristics of damage in beams.

Tested Damage Scenarios

To verify the efficiency and accuracy of the proposed baseline-free damage identification algorithm for beam structures, a total of three damage scenarios were tested for small-scale damage, i.e., 3 mm, with different sensor locations, as depicted in Table 1. For damage scenarios SS1 (single damage 1), DS1 (double damage 1) and TS1 (triple damage 1) all sensors are located at 16 specified locations. In DS2 scenario, fifteen sensors are distributed at points 1–16, except point number 13. The purpose of DS2 is to verify that the proposed algorithm does not indicate any false alarm when the sensor is not located at the damage location. In addition, the TS2 scenario with the fifteen numbers of sensors deployed (see Table 1), demonstrate the influence of sensor position in identification of damage location.

Genetic Algorithm

GA is an optimization method that simulates the natural evolution phenomena inspired by Darwin's survival-of-the-fittest theory. In this optimization method, information about a problem, such as variable parameters, is coded into a genetic string

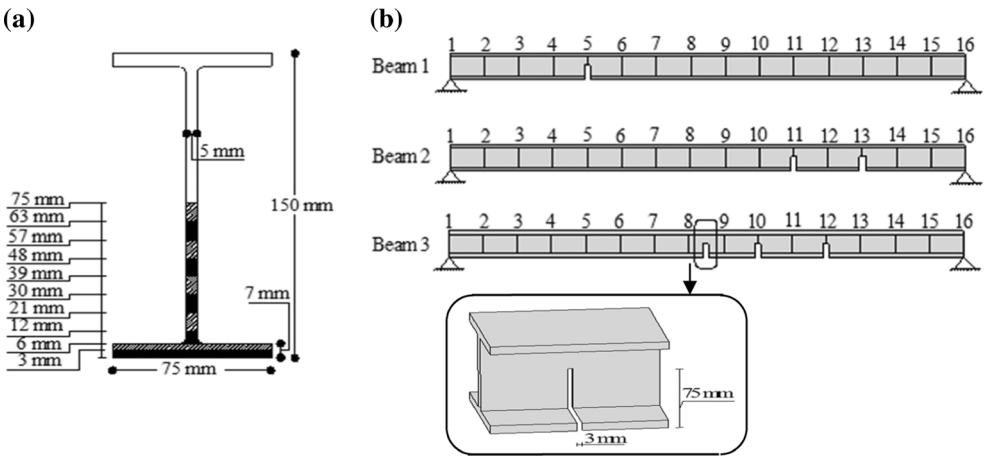

Fig. 2 (**a**) Cross section of tested beams, (**b**) dimensions and damage locations of tested beams

Table 1 Various sensor deployments on damaged beams

Damage type	Damage scenario		Sensor location
Notch cutting	Single	SS1	1, 2, 3, 4, 5, 6, 7, 8, 9, 10, 11, 12, 13, 14, 15, 16
	Double	DS1	1, 2, 3, 4, 5, 6, 7, 8, 9, 10, 11, 12, 13, 14, 15, 16
		DS2	1, 2, 3, 4, 5, 6, 7, 8, 9, 10, 11, 12, 14, 15, 16
	Triple	TS1	1, 2, 3, 4, 5, 6, 7, 8, 9, 10, 11, 12, 13, 14, 15, 16
		TS2	1, 2, 3, 4, 5, 6, 7, 8, 10, 11, 12, 13, 14, 15, 16

known as the chromosome. Each of these individuals has an associated fitness value, which is usually determined by the fitness function to be maximized or minimized [32, 46]. In a GA, a population of individuals is created by randomly generating a set of candidate solutions and encoding these solutions into binary strings. Each individual in the population then undergoes evaluation and is assigned a fitness value based on how well the individual satisfies the state objective. Generally, GA consists of three operations: (1) parent selection, (2) crossover, and (3) mutation.

In this study, the tournament selection for choosing the solution pairs of the reproduction stage has been adopted among the selection operators [47] and two-point crossover was employed for every chromosome of the chromosome-pair with a 50 % probability of selection. The two parents selected for crossover were in charge of exchanging information that lies between two randomly generated points within the binary string.

The successful application of GAs to a problem is significantly reliant on detecting an appropriate method for chromosome encoding. The success of the training process is important for the creation of a fitness function to rank the performance of a specific chromosome [32]. The genetic algorithm rates its own performance with respect to that of the fitness function. Consequently, the generic algorithm would be unable to achieve the requirements of the users unless the fitness function adequately takes account of the desired performance features.

In the proposed algorithm, the GA was employed in order to search for the optimal Daubechies order and decomposition level of the signals by means of the fundamental fitness function as:

$$\max Fit = \left\| 1 - \frac{mean\left(F_{RWPE}^{\gamma}\right)}{\sum_{k=1}^{nd} RF_k^{\beta}} \right\|_2 \tag{14}$$

where $\|\cdot\|_2$ is the Euclidean norm, γ is number of sensor locations ($\gamma = 1, 2, \ldots, N$)), RF is the baseline-free damage indicator, F_{RWPE}, at identified location β, ($\beta = 1, 2, \ldots, k$), and k is the number of damage locations.

The procedure of employing GA begins by defining a chromosome, i.e., an array of variables whose values are to be optimized. The proposed chromosomes contained five genes for the Daubechies mother wavelet function and three genes for the decomposition level of signals, as shown in Fig. 3. The fitness function generates an output from the set of input variables of a chromosome. These chromosomes undertake genetic operations to produce next generation chromosomes. This process is repeated until the convergence condition is reached. The convergence condition is obtained when either the best chromosome has not changed for a number of generations or the number of generations reaches its given maximum value.

Figure 4 depicts the general scheme of damage identification optimization. In addition, Tables 2 and 3 present the parameters and variables of the GA used in the research, respectively.

Baseline-Free Damage Identification Result

Damage Location Identification

The applicability of the proposed baseline-free damage identification algorithm is validated with several considered damage scenarios, shown in Table 1. With regard to the identification of damage location in the single damage scenario, SS1, by running the GA, DB2 and level 5 have been selected as the best values for Daubechies order and decomposition level, respectively, and subsequently the F_{RWPE} values for every point are calculated, as depicted in Fig. 5(a). It can be observed that the magnitude of F_{RWPE} at point 5 was greater than those from the other locations corresponding to the exact damage location. To determine the damage location distinctly, the threshold value for damage indicators were established through applying the statistical properties and the one-side confidence limit of the F_{RWPE} values. With a 98 % confidence

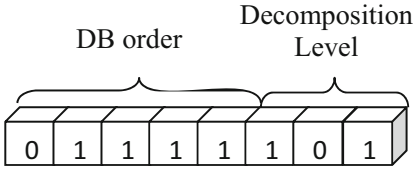

Fig. 3 Proposed chromosome for GA

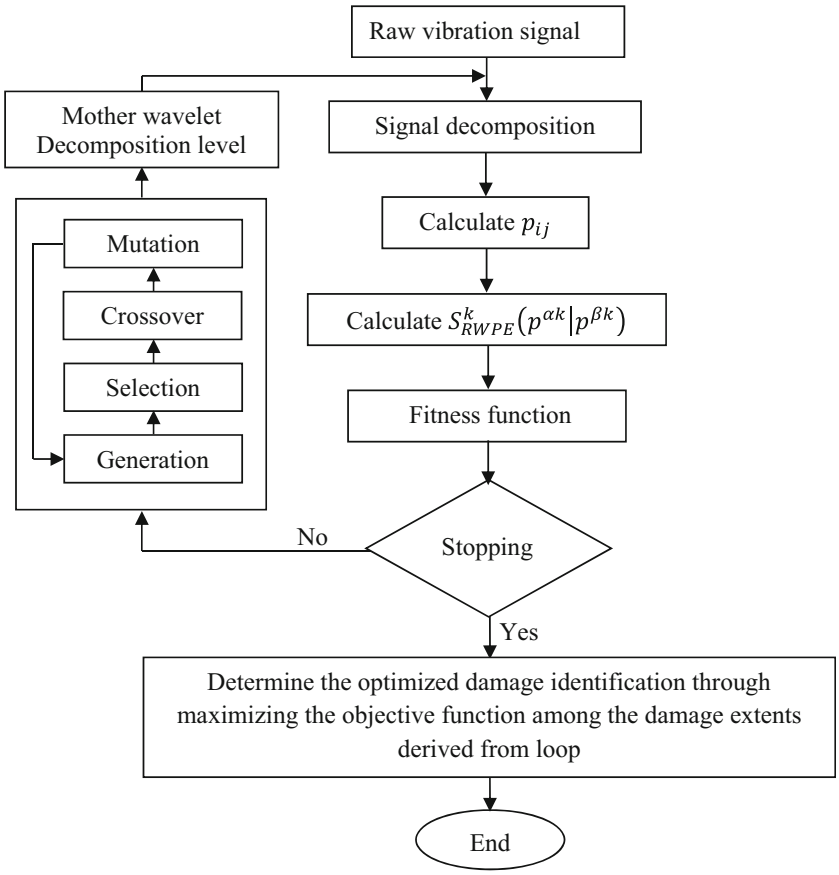

Fig. 4 General scheme of algorithm optimization for damage identification

interval ($\overline{\alpha} = 0.02$), the histogram of F_{RWPE} values after considering the damage threshold for SS1 damage scenario is depicted in Fig. 5(b). It is evident that the F^{UL}_{RWPE} arise at sensor location 5, which indicates the actual damage location.

In addition, the sensitivity of results are confirmed by comparing the F_{RWPE} values before and after the damage in SS1 damage scenario, as illustrated in Fig. 5(c). The significant increase in the F_{RWPE} was depicted at the damage location. Thus, the indicator F_{RWPE} is considered an effective measure in the proposed damage detection algorithm.

In the multi-damage cases, the optimal DB order and decomposition level corresponding to each damage scenario have been selected by using GA, as shown in Table 3. In addition, the results of double and triple scenarios with various number of sensor locations were presented in Fig. 6. It can be observed that, in DS1 damage scenario, Fig. 6(a), the F^{UL}_{RWPE} arises clearly at sensor locations 11 and 13, which coincide with real damage locations. As indicated in Fig. 6(b), when the sensors were not located at damage location 13, no peak was observed in F_{RWPE} values to indicate the damage location 13. The histogram of F^{UL}_{RWPE} with consideration of damage threshold values obtained from equation (13) is depicted in Fig. 6(b). From this figure, it can be seen that only the sensor in location 11 was able to successfully identify the location of damage. In addition, comparison of the peak values of F^{UL}_{RWPE} in DS1 damage scenario, reveals that larger intensity of the F^{UL}_{RWPE} occurs when the damage was located near the center of the beam since the local perturbations caused by the damage, take place at a far distance from the support. On the other hand, the presence of damage adjacent to the support results in a singularity around the support, which can reduce the accuracy of the identification.

Table 2 GA parameters

Number of generation	200
Population	30
Selection function	Tournament
Fitness normalization	Rank
Crossover	$Pc = 0.7$, Single-point, uniform
Mutation	$Pm = 0.2$, Uniform

Table 3 GA variables

Variable name	Range	Optimized value		
		Beam1	Beam2	Beam3
Daubechies order	DB1-DB31	DB2	DB5	DB15
Decomposition level	2–7	5	5	6

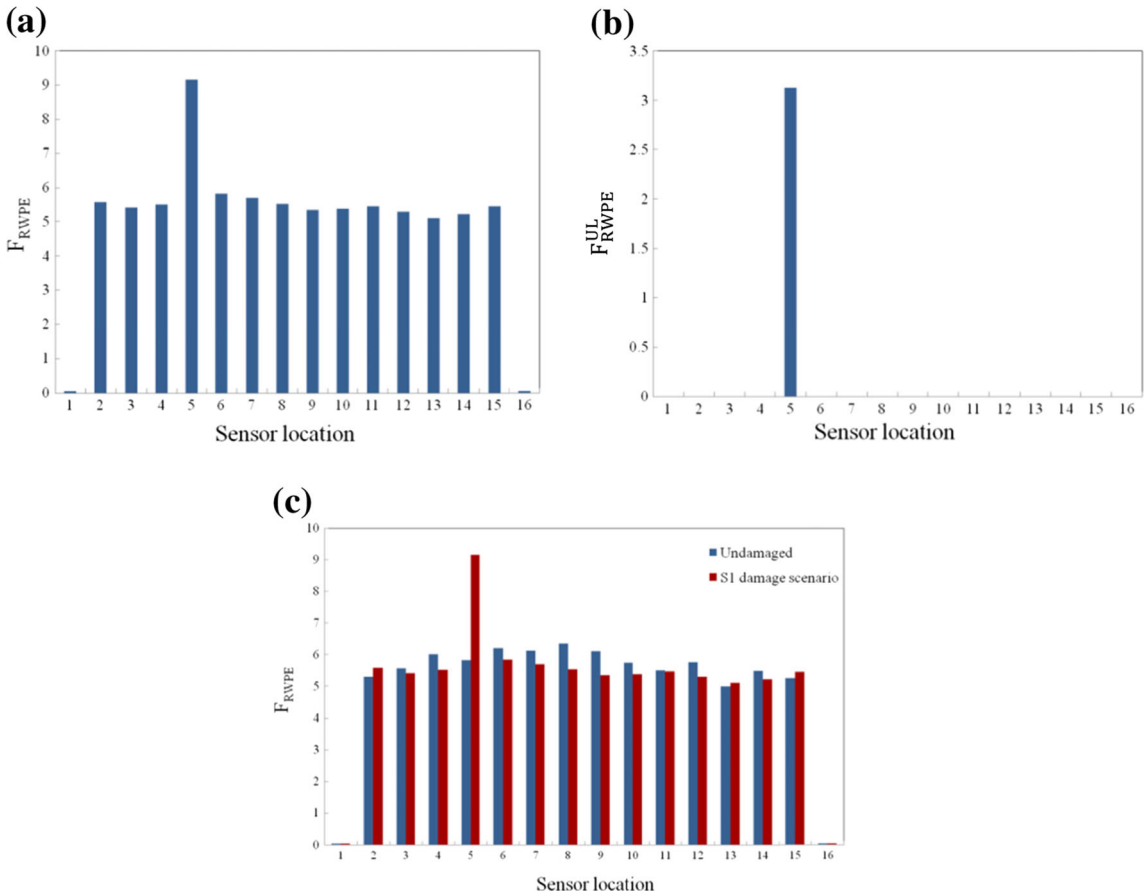

Fig. 5 Damage identification in beam1, (**a**) histogram of F_{RWPE}, (**b**) histogram of F^{UL}_{RWPE} after consider damage threshold, (**c**) comparison of F_{RWPE} before and after damage

The results of triple damage scenarios with different number of sensors were also presented in Fig. 6(c) and (d), respectively. Based on the result in TS1 damage scenario shown in Fig. 6(c), it can be seen that the F^{UL}_{RWPE} arise at location 8,9,10 and 12, which coincided with damage locations. In addition, the results indicated that the F^{UL}_{RWPE} for sensor locations 8 and 9 have lower intensity and sensitivity relative to the sensor location 10, even though they were located in the middle of the beam span. The reason for such behavior was caused by the influence of damage and signal attenuation, when it was located adjacent to sensor locations the signal attenuates and a part of signal energy decays once it was recorded by the sensor. As shown in Fig. 6(d), the TS2 damage scenario with fifteen sensor deployment could also successfully identify the damage locations.

By comparing the results, it can be demonstrated that, the F^{UL}_{RWPE} value at damaged location for single damage scenario (Fig. 5) was considerably larger than the one for triple damage scenario (Fig. 6). It means that as the number of damage locations increases, the number of sensors were also required to increase in order to secure sufficient specificity for identifying multiple damage locations.

Identification of Progressive Damage

The verification of the proposed algorithm was also carried out with progressive damage scenarios of the simulated simply-supported beams from the small-scale damage. Figure 7 shows the values of indicators F^{UL}_{RWPE} calculated according to equation (12) for beam 1 with a single damage scenario. By using the GA, DB2 and level 5 were selected as the best values for the Daubechies order and decomposition level, respectively. Figure 7 clearly depicts the difference between various orders of Daubechies to discriminate the location and severity of damage. As can be seen, the damage locations were distinguishable in these histograms with F^{UL}_{RWPE} reaching a maximum value at location 5 which was the exact damage location. However, the peak of F^{UL}_{RWPE} was not as clearly distinguishable in DB15 even though it had the same location and severity of damage. Furthermore, the changes in values of F^{UL}_{RWPE} for each depth of damage were not as comparable to DB2. For DB11, the shortcomings were identical to that of DB15 but gave more appropriate results. DB5 was not a worthy consideration since it was not able to precisely indicate the damage location. It is significant to note

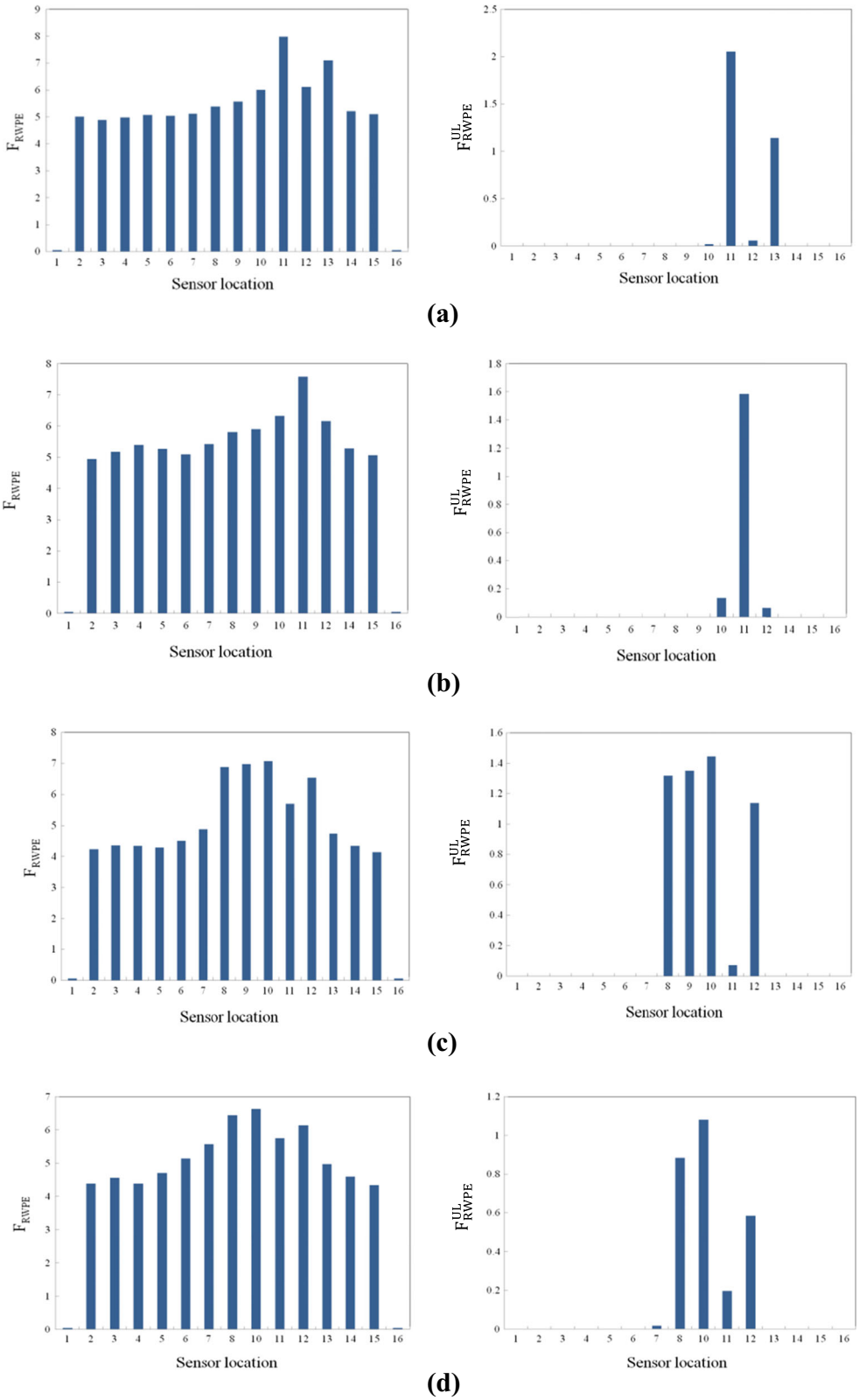

Fig. 6 Damage identification in multiple damage scenarios with different sensor locations, (**a**) DS1, (**b**) DS2, (**c**) TS1, (**d**) TS2

that the accuracy of differentiating the damage cannot be compared to DB2 for the single damage scenario.

In order to clarify the estimated values, the performance of the fundamental fitness function at the fifth level of

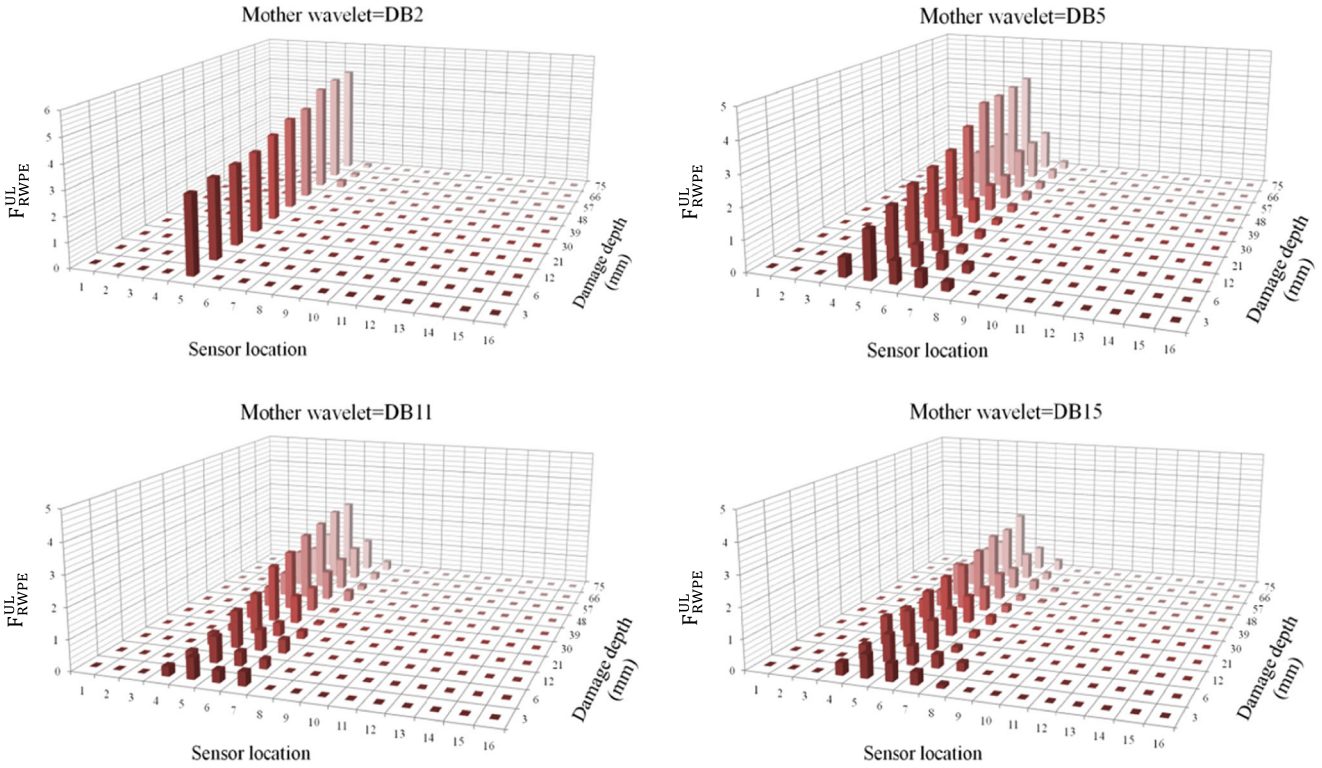

Fig. 7 Histograms of F^{UL}_{RWPE} in beam1 with different Daubechies orders

decomposition was also calculated manually through the percentage of standard difference between the F_{RWPE} values at damage locations and average of the remaining points ($[(\sum_i F^{max}_{RWPE} - \sum F^{ave}_{RWPE})/\sum F^{ave}_{RWPE})] \times 100$; i = number of damage scenarios) at every specific depth of damage. The results are tabulated in Table 4. Comparison of each column associated with every depth of damage for all the considered DBs indicates that from manual calculations, wavelet function DB2 was the suitable wavelet function order. This coincides with the outcome of GA estimation. For instance, in the case of 30 mm damage depth, the maximum value of standard difference was associated with DB2 by 90.10 % compared to other DBs. A similar trend was observed for other considered damage depths.

To extract the relevant information from Table 4 for all DBs in each depth of damage, the one-way ANOVA followed by Duncan's multiple-range test were employed. Significant differences between DBs ($F = 23.43$, $p < 0.01$) and DB2 were found in the statistical analysis. The results revealed that the mean of DB2 ($M = 50.82$) was significantly greater than other DBs.

In beam 2, the GA was utilized to identify the most accurate location and severity of damage by maximizing the fitness function. The outcome of the GA analysis which is depicted in Fig. 8 revealed that DB5 with 5 level of decomposition performed better in two damage scenarios compared to other Daubechies orders. Firstly, by comparing the considered Daubechies orders shown in Fig. 8, it can be seen that for DB11, the damage locations were not easily identified while DB5 clearly identified damage locations 11 and 13 together with appropriate representation by the histograms i.e., values of F^{UL}_{RWPE} at damage locations compared to other Daubechies orders. Meanwhile, by scrutinizing the histograms, the damage locations in DB2 and DB15 could be identified. In addition, from the histograms it can be observed that the intensity of F^{UL}_{RWPE} at location 11 was relatively larger than location 13 although both have similar damage severity. This is possibly due to location 11 being close to the middle of the beam while location 13 was close to the support.

For beam 3 with multiple damages, DB15 with 6 level of decomposition was found to be the appropriate DB order for damage identification. The advantage of DB15 compared to other Daubechies orders was that the value of F^{UL}_{RWPE}, as shown in Fig. 9, precisely shows the damage locations along the beam length. The intensity of F^{UL}_{RWPE} was influenced by the notch locations as well as the distance from the supports. The corresponding intensity of F^{UL}_{RWPE} for the damage located at the middle of the beam is expected to be larger than those closer to the support. However, due to the signal attenuation effect raised by the presence of damage between two sensor locations, the intensity of F^{UL}_{RWPE} of the damage between locations 8 and 9 is lower than that of location 10.

To verify the estimated values, Table 5 shows the mean values of standard difference percentage of F_{RWPE} values

Table 4 Daubechies wavelets comparison for each damage depth for beam 1

Wavelet function order	Standard difference (%)										
	Damage depth (mm)										Mean*
	3	6	12	21	30	39	48	57	66	75	
DB 2	28.74	28.12	36.13	41.41	46.08	59.43	59.54	70.10	69.40	69.34	**50.83a**
DB 3	14.51	15.11	17.27	18.33	23.81	23.34	27.75	26.79	26.37	27.78	22.11cdef
DB 4	13.09	14.87	15.72	17.16	23.73	25.39	27.49	25.50	24.34	26.64	21.39cdef
DB 5	20.09	30.34	23.64	26.77	34.09	40.68	46.92	42.29	41.83	41.97	34.86b
DB 6	14.08	13.32	18.80	18.31	19.92	20.53	28.24	29.37	28.57	28.94	22.01cdef
DB 7	13.11	13.05	14.17	16.18	16.62	17.35	19.45	19.85	17.70	19.98	16.75fgh
DB 8	6.45	7.96	10.85	10.54	11.15	12.63	14.17	13.06	15.72	15.47	11.8 h
DB 9	9.97	9.87	12.01	13.14	14.19	16.69	16.40	17.13	20.06	19.97	14.94gh
DB 10	15.13	15.67	15.42	18.23	27.16	27.26	30.30	31.34	30.39	31.52	24.24 cd
DB 11	17.94	19.22	24.37	22.79	30.23	31.82	35.45	31.80	29.61	29.99	27.32c
DB 15	17.45	17.09	20.73	21.90	26.39	26.86	26.67	25.53	24.99	26.59	23.42cde
DB 16	12.99	12.90	13.23	14.35	18.01	18.28	20.82	20.97	19.26	21.58	17.24efgh
DB 17	14.19	13.88	13.97	15.16	19.55	19.72	21.38	23.80	23.07	23.79	18.85defg
DB 18	9.64	11.31	12.19	12.21	12.54	12.46	13.87	12.92	12.94	13.38	12.34 h
DB 19	8.36	9.68	11.81	12.37	12.20	13.34	15.73	15.78	15.39	15.84	13.05gh
DB 20	14.50	15.84	15.26	21.73	23.56	23.22	30.22	31.14	29.98	31.36	23.68 cd
DB 21	10.29	11.53	12.00	12.00	13.12	13.04	13.80	14.48	13.38	13.89	12.75gh

* Mean values with the same letter were not significantly different

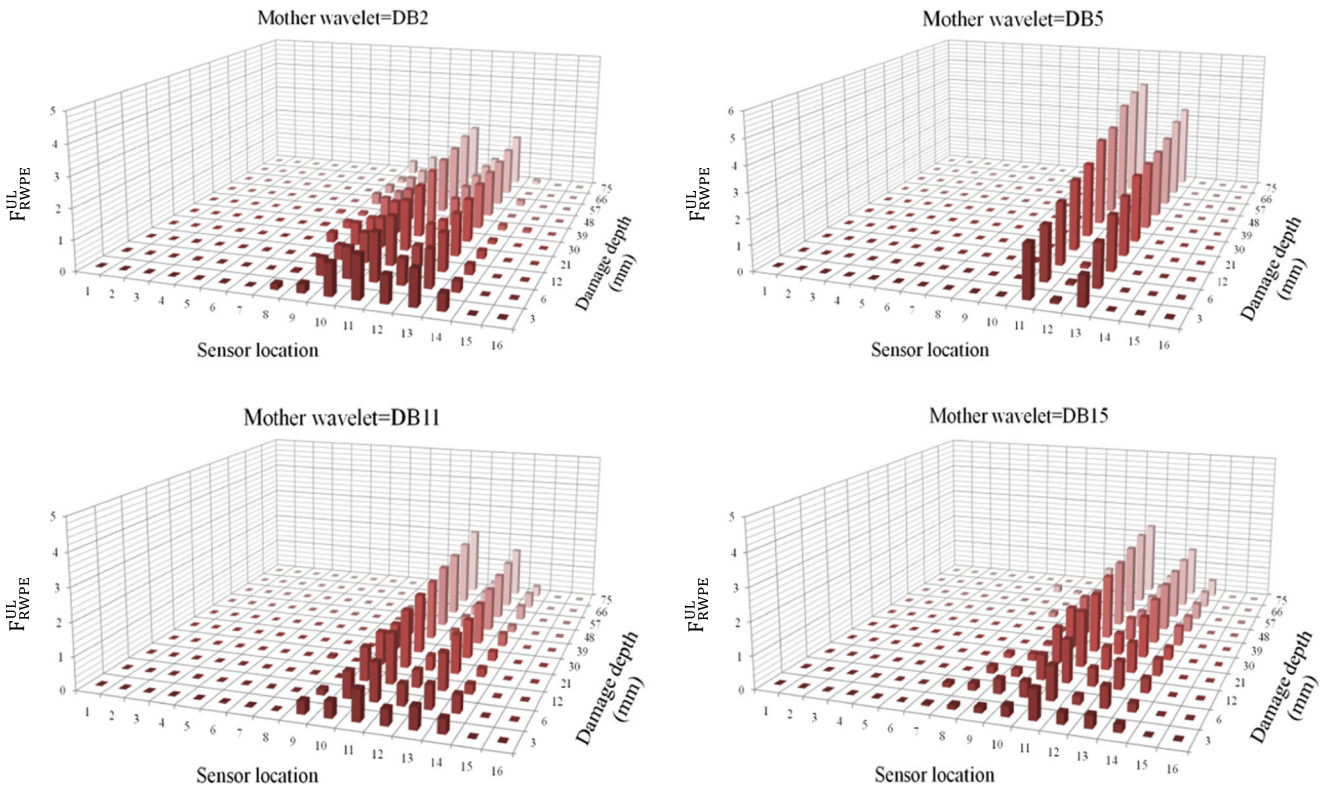

Fig. 8 Histograms of F^{UL}_{RWPE} in beam 2 with different Daubechies orders

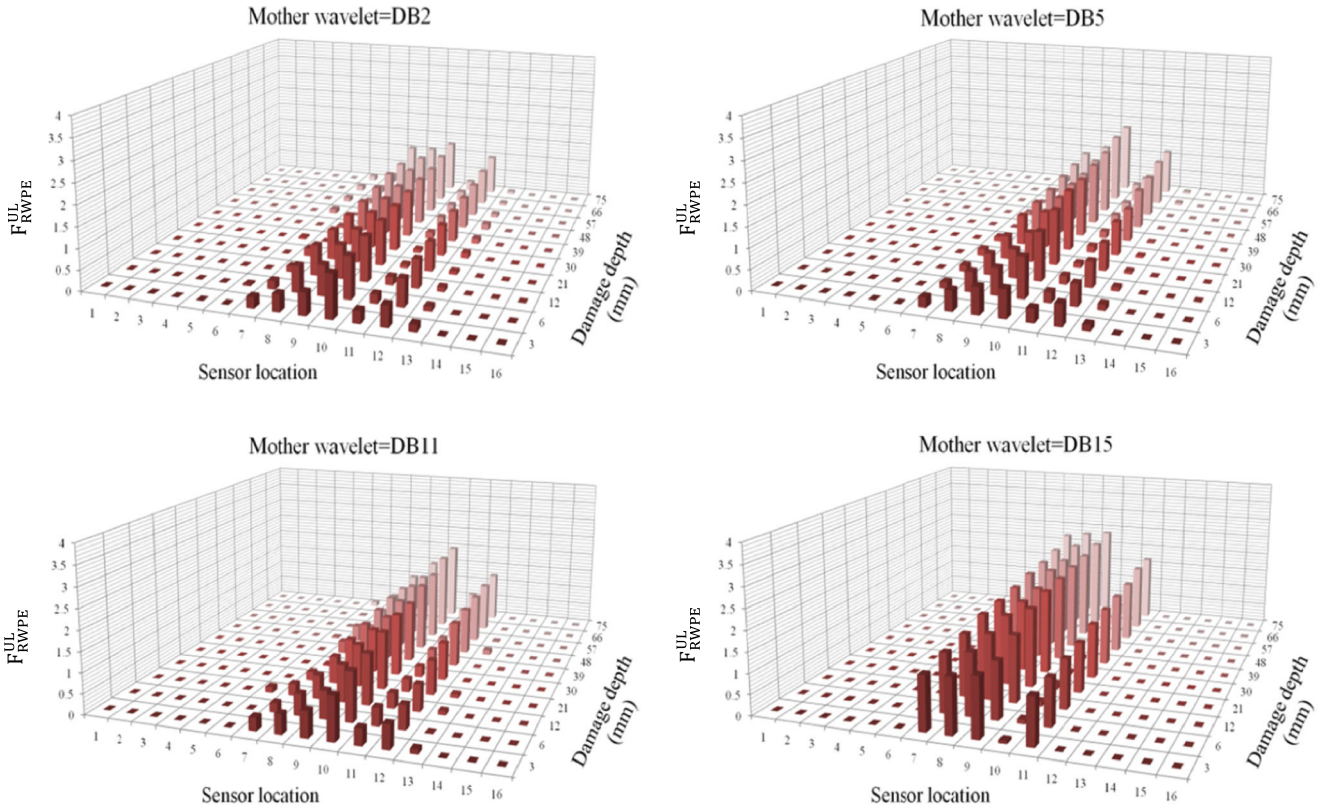

Fig. 9 Histograms of F^{UL}_{RWPE} in beam 3 with different Daubechies orders

Table 5 Daubechies wavelets comparison for multiple damage scenarios

Wavelet function order	Mean*	
	Beam 2	Beam 3
DB 2	179.67bc	450.22cde
DB 3	158.36def	426.83ef
DB 4	156.84ef	397.60 g
DB 5	**223.12a**	462.16c
DB 6	166.28cdef	447.53cde
DB 7	153.57f	435.12de
DB 8	173.07bcd	441.83cde
DB 9	168.26 cdef	450.44cde
DB 10	167.76cdef	456.26 cd
DB 11	169.38bcde	494.83b
DB 15	181.18bc	**531.31a**
DB 16	163.28def	432.90de
DB 17	162.98def	433.85de
DB 18	158.54def	442.19cde
DB 19	162.21def	407.38 fg
DB 20	182.88b	496.71b
DB 21	166.30cdef	457.11 cd

*Mean values with the same letter were not significantly different

for multiple damage scenarios at specified level of decomposition without using GA. Analysis performed by ANOVA indicated the significant differences among the DB5 and DB15 with other DBs in each damage scenario. Comparison of results showed that the mean value of DB5 and DB15 are considerably greater than other DBs in each damage scenario. Hence, it can be inferred that not only does the GA has the potential to verify the proposed algorithm to obtain the optimal solution but also provides evidence for the accuracy of the parameters for adjustment of the algorithm.

Results have demonstrated that the locations of notches can be successfully determined from the measured time history acceleration responses through variation of F^{UL}_{RWPE}. In addition, the respective amplitude levels of the histograms can be used as a criterion to identify severity of damage, although not quantitatively. Therefore, selection of a proper mother wavelet for wavelet-based methods is crucial to improve the performance of the proposed method in order to achieve accurate results. The type of mother wavelet function plays a key role in reducing the false positives adjacent to damage locations, as depicted in Figs. 7, 8 and 9. This is mostly because the correlation between the mother wavelet functions and the signal is calculated as a wavelet coefficient and this is the significance of the proposed method.

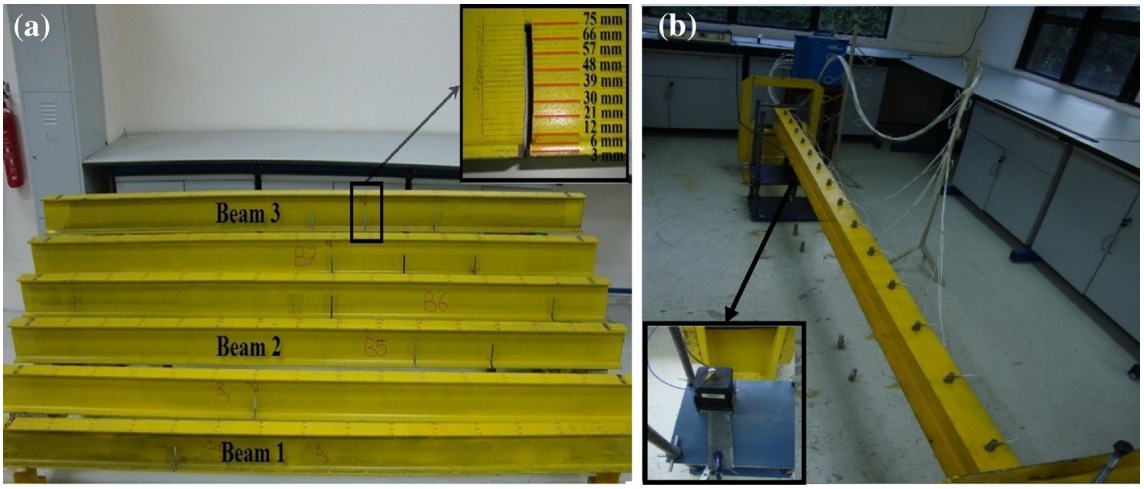

Fig. 10 (**a**) Damage locations of tested beams. (**b**) Experimental setup and data acquisition system

Experimental Verification

Experimental Setup

To validate the proposed algorithm by experimental data where measurement error and noise are present, vibration tests were performed on three I-section steel beams with different damage scenarios. Beams with a 3 m span length, as shown in Fig. 10, with damage at the designated locations described in Table 6 were considered. The damage was induced by introducing a saw cut at the prescribed locations on the beam with varying depth of cut.

The analogue data from the sensors is converted via an analysis digital center using the OROS OR35 analyzer. The signal analyzer is capable of generating all the different forms of signals, including white noise which was used in this test. The beam was excited using a shaker at node 14. The acceleration response of the K-shear Kistler accelerometers was measured at sixteen locations on the top flange along the beam (Fig. 10(b)). These accelerometers have a frequency range of 0.5–10 kHz and a sensitivity of 100 mV/g.

The time history signal of the shaker and the accelerometers were amplified and response signals were processed by the analyzer. Figure 11 shows the front end of the analyzer with sixteen accelerometers connected to channel 4–20 and channel 21 was used for the force transducer. The sampling rate was set to 5.12 kS/s to achieve a frequency bandwidth of 2000 Hz.

Table 6 Damage scenarios

Damage case	Damage scenario	Damage point	Width of damage (mm)	Depth of damage (mm)
Beam 1	Single	5	3	3 up to 75
Beam 2	Double	11,13	3	3 up to 75
Beam 3	Multiple	Middle of beam, 10,12	3	3 up to 75

Experimental Results

The following observations were made based on the structural response signal of damaged beams. By running the GA on the first damage case i.e., beam 1 with a single damage as shown in Fig. 12(a), Daubechies order 2 and decomposition level 6 were chosen as the best parameters for the adjustment of the algorithm for differentiating the damages. The damage location at position 5 could be clearly identified with the significant change in values of F^{UL}_{RWPE}. In beam 2 with the double damage scenario as depicted in Fig. 12(b), the influence of changing the wavelet function as well as level of decomposition on the accuracy of damage identification was investigated by using the GA. As a consequence, Daubechies wavelet function with order of 5 and decomposition level 6 were selected as the best function for identification of damage

Fig. 11 Front end of analyzer

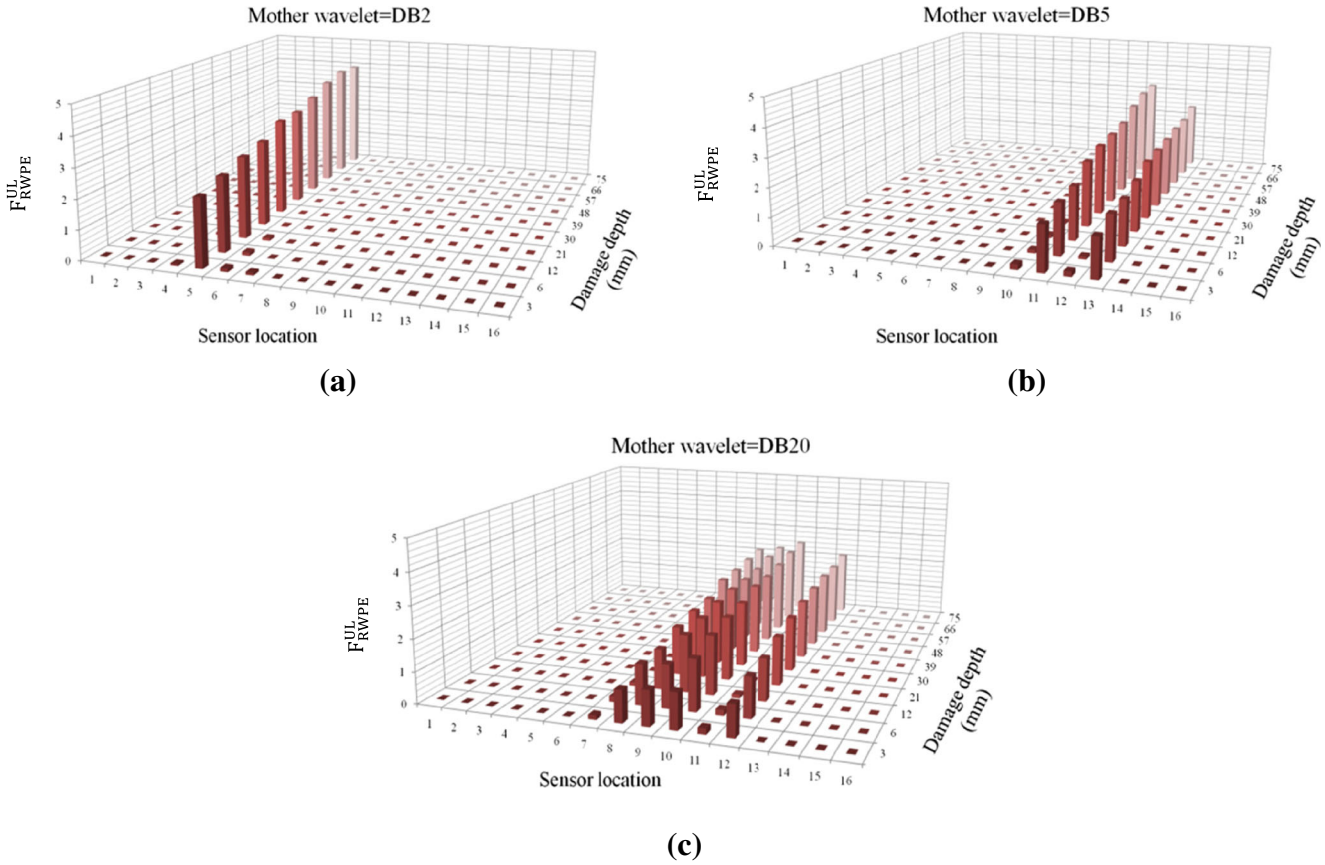

Fig. 12 Histograms of F^{UL}_{RWPE} in (**a**) beam 1, (**b**) beam 2, and (**c**) beam 3 with different Daubechies orders

location and severity. Furthermore, the intensity of F^{UL}_{RWPE} at damage location 11 which was located at the middle of the beam were slightly higher than that of damage location 13 which may be due to its close distance to the support. In beam 3 with the multiple-damage scenarios as shown in Fig. 12(c), Daubechies order 20 and decomposition level 6 were selected as the suitable function by GA and both damage locations and severities could be identified. However, for the whole set of data, the maximum value of the F^{UL}_{RWPE} was always detected at the exact damage location.

The results have demonstrated that for wavelet-based methods, the choice of the mother wavelet function is of paramount importance to improve the performance of the algorithm. However, as indicated in this study, it is possible to have satisfactory algorithm performance with a particular mother wavelet function. Moreover, from the comparison of histograms in different damage scenarios, the values of F^{UL}_{RWPE} were found to be proportional to damage severity. Therefore, this damage indicator can be used to quantify the damage severity. Also, by comparing results corresponding to the damage cases, it can be seen that changes in damage location causes a scenario which requires a different suitable mother wavelet function. Hence, the final outcome obtained from GA was found to have great potential to determine the optimal solution and to investigate the reliability of the parameters for algorithm adjustment.

In addition, varying operational and environmental conditions of the structure raise a discrepancy, i.e., false alarm, which is reduced because of the baseline-free nature of the proposed method. Since all sensors are subjected to the same environmental condition and measured the vibration signals at the same time. Thus the vibration signals measured at a location can act as reference signals to other location that has comparable structural feature.

Conclusions

An intelligent damage identification algorithm to detect damage in beam-like structures using vibration signal was developed and implemented. To verify the efficiency and practicability of the method proposed in the current research, both numerical simulation and experimental tests were carried out. The baseline-free damage indicator was defined from an optimized wavelet packet transform which was combined with the information entropy to gain the advantages of both techniques. Results conclude that the wavelet-based techniques are absolutely dependent of the mother wavelet

function. On the other hand, the most inevitable challenge in wavelet analysis for damage identification as shown in previous research works has been the determination of mother wavelet function and decomposition level through trial and error based on intrinsic characteristics of the data. This has limited earlier researches to use a specific mother wavelet function and decomposition level for various damage scenarios of beam-like structures. However, the novelty of the proposed method is using various mother wavelet functions and decomposition levels for every damage scenario at different locations. The mother wavelet and decomposition level are optimally chosen by GA which can resolve the problem of baseline-free methods. The baseline-free methods suffer from presence of multiple-damage scenario in several locations throughout a beam. Therefore, the difficulty in implementation of mother wavelet function through trial-and-error based methods is eliminated. Also, all the results show that the optimal damage indicator can be successfully used to identify the damage locations as well as damage severity from the response data of the damaged beam using an effective comparative approach. The results demonstrated that the proposed algorithm has great potential and considerable accuracy for damage identification in beam-like structures.

Acknowledgements The authors would like to express their sincere thanks to the Ministry of Education, Malaysia for the support given through research grants PG222-2014B and UM.C/625/1/HIR/MOHE/ENG/55.

References

1. Farrar C, Worden K (2007) An introduction to structural health monitoring. Phil Trans R Soc A 365(1851):303–315
2. Farrar C, Doebling S, Nix D (2001) Vibration–based structural damage identification. Phil Trans R Soc A 359(1778):131–149
3. Fan W, Qiao P (2011) Vibration-based damage identification methods: a review and comparative study. Struct Health Monit 10(1):83–111
4. Kim H, Melhem H (2004) Damage detection of structures by wavelet analysis. Eng Struct 26(3):347–362
5. Chang C-C, Chen L-W (2003) Vibration damage detection of a Timoshenko beam by spatial wavelet based approach. Appl Acoust 64(12):1217–1240
6. Chang C-C, Chen L-W (2004) Damage detection of cracked thick rotating blades by a spatial wavelet based approach. Appl Acoust 65(11):1095–1111
7. Chang C-C, Chen L-W (2005) Detection of the location and size of cracks in the multiple cracked beam by spatial wavelet based approach. Mech Syst Signal Proc 19(1):139–155
8. Gentile A, Messina A (2003) On the continuous wavelet transforms applied to discrete vibrational data for detecting open cracks in damaged beams. Int J Solids Struct 40(2):295–315
9. Loutridis S, Douka E, Trochidis A (2004) Crack identification in double-cracked beams using wavelet analysis. J Sound Vib 277(4): 1025–1039
10. Umesha P, Ravichandran R, Sivasubramanian K (2009) Crack detection and quantification in beams using wavelets. Comput-Aided Civil Infrastruct Eng 24(8):593–607
11. Ovanesova A, Suarez L (2004) Applications of wavelet transforms to damage detection in frame structures. Eng Struct 26(1):39–49
12. Bagheri A, Li K, Rizzo P (2013) Reference-free damage detection by means of wavelet transform and empirical mode decomposition applied to Lamb waves. J Intell Mater Syst Struct 24(2):194–208
13. Chang C-C, Chen L-W (2004) Damage detection of a rectangular plate by spatial wavelet based approach. Appl Acoust 65(8):819–832
14. Rucka M, Wilde K (2006) Application of continuous wavelet transform in vibration based damage detection method for beams and plates. J Sound Vib 297(3):536–550
15. Wang Q, Deng X (1999) Damage detection with spatial wavelets. Int J Solids Struct 36(23):3443–3468
16. Zhong S, Oyadiji S (2007) Crack detection in simply supported beams without baseline modal parameters by stationary wavelet transform. Mech Syst Signal Process 21(4):1853–1884
17. Zhong S, Oyadiji S (2011) Detection of cracks in simply-supported beams by continuous wavelet transform of reconstructed modal data. Comput Struct 89(1):127–148
18. Lee S, Yun G, Shang S (2014) Reference-free damage detection for truss bridge structures by continuous relative wavelet entropy method. Struct Health Monit 1475921714522845
19. Mikami S, Beskhyroun S, Oshima T (2011) Wavelet packet based damage detection in beam-like structures without baseline modal parameters. Struct Infrastruct Eng 7(3):211–227
20. Castro E, Garcia-Hernandez M, Gallego A (2006) Damage detection in rods by means of the wavelet analysis of vibrations: influence of the mode order. J Sound Vib 296(4):1028–1038
21. Castro E, Garcia-Hernandez M, Gallego A (2007) Defect identification in rods subject to forced vibrations using the spatial wavelet transform. Appl Acoust 68(6):699–715
22. Spanos P, Failla G, Santini A, Pappatico M (2006) Damage detection in Euler–Bernoulli beams via spatial wavelet analysis. Struct Control Health Monit 13(1):472–487
23. Inoue H, Kishimoto K, Shibuya T (1996) Experimental wavelet analysis of flexural waves in beams. Exp Mech 36(3):212–217
24. Kim H, Melhem H (2003) Fourier and wavelet analyses for fatigue assessment of concrete beams. Exp Mech 43(2):131–140
25. Han J-G, Ren W-X, Sun Z-S (2005) Wavelet packet based damage identification of beam structures. Int J Solids Struct 42(26):6610–6627
26. Ren W-X, Sun Z-S (2008) Structural damage identification by using wavelet entropy. Eng Struct 30(10):2840–2849
27. Yam L, Yan Y, Jiang J (2003) Vibration-based damage detection for composite structures using wavelet transform and neural network identification. Compos Struct 60(4):403–412
28. Diao Y-S, Li H-J, Wang Y (2006) A two-step structural damage detection approach based on wavelet packet analysis and neural network. Proceedings of the 5th International Conference on Machine Learning and Cybernetics 3128–3133
29. Law S, Li X, Zhu X, Chan S (2005) Structural damage detection from wavelet packet sensitivity. Eng Struct 27(9):1339–1348
30. Cruz P, Salgado R (2009) Performance of vibration-based damage detection methods in bridges. Comput Aided Civil Infrastruct Eng 24(1):62–79
31. Vafaei M, Adnan A, Abd Rahman A (2014) A neuro-wavelet technique for seismic damage identification of cantilever structures. Struct Infrastruct Eng (ahead-of-print) 1–19
32. Haupt R, Haupt S (2004) John Wiley & Sons, New Jersey, USA
33. Hao H, Xia Y (2002) Vibration-based damage detection of structures by genetic algorithm. J Comput Civil Eng 16(3):222–229
34. Vakil-Baghmisheh M-T, Peimani M, Sadeghi M, Ettefagh M (2008) Crack detection in beam-like structures using genetic algorithms. Appl Soft Comput 8(2):1150–1160

35. Rafiee J, Tse P, Harifi A, Sadeghi M (2009) A novel technique for selecting mother wavelet function using an intelli gent fault diagnosis system. Expert Syst Appl 36(3):4862–4875
36. Neild S, McFadden P, Williams M (2003) A review of time-frequency methods for structural vibration analysis. Eng Struct 25(6):713–728
37. Mallat S (1999) A wavelet tour of signal processing. Academic, New York, USA
38. Daubechies I (1992) Ten lectures on wavelets. SIAM, Philadelphia, USA
39. Ren W-X, Sun Z-S, Xia Y, Hao H, Deeks A (2008) Damage identification of shear connectors with wavelet packet energy: laboratory test study. J Struct Eng 134(5):832–841
40. Shinde A, Hou Z (2005) A wavelet packet based sifting process and its application for structural health monitoring. Struct Health Monit 4(2):153–170
41. Sun Z, Chang C-C (2007) Vibration based structural health monitoring: wavelet packet transform based solution. Struct Infrastruct Eng 3(4):313–323
42. Taha M, Noureldin A, Lucero J, Baca T (2006) Wavelet transform for structural health monitoring: a compendium of uses and features. Struct Health Monit 5(3):267–295
43. Yen G, Lin K-C (2000) Wavelet packet feature extraction for vibration monitoring. IEEE Trans Ind Electron 47(3):650–667
44. Rosso O, Martin M, Figliola A, Keller K, Plastino A (2006) EEG analysis using wavelet-based information tools. J Neurosci Methods 153(2):163–182
45. Xia Y, Hao H, Deeks A (2005) Vibration-based damage detection of shear connectors in Nickol river bridge and Balla Balla river bridge. Part II: laboratory study. Australia: School of Civil & Resource Engineering. The University of Western Australia. Australia: School of Civil & Resource Engineering, The University of Western Australia, Report No. ST-05-02
46. Goldberg D, Holland J (1988) Genetic algorithms and machine learning. Mach Learn 3(2):95–99
47. Rao M, Srinivas J, Murthy B (2004) Damage detection in vibrating bodies using genetic algorithms. Comput Struct 82(11):963–968